REMOTE SENS. ENVIRON. 50:255–266 (1994)

Mapping and Monitoring Conifer Mortality Using Remote Sensing in the Lake Tahoe Basin

Scott A. Macomber and Curtis E. Woodcock**

A prolonged drought in the western United States has resulted in alarming levels of mortality in conifer forests. Satellite remote sensing holds the potential for mapping and monitoring the effects of such environmental changes over large geographic areas in a timely manner. Results from the application of a forest canopy reflectance model using multitemporal Landsat TM imagery and field measurements, indicate conifer mortality can be effectively mapped and inventoried. The test area for this project is the Lake Tahoe Basin Management Unit in the Sierra Nevada of California. The Landsat TM images are from the summers of 1988 and 1991. The Li–Strahler canopy model estimates several forest stand parameters, including tree size and canopy cover for each conifer stand, from reflectance values in satellite imagery. The difference in cover estimates between the dates forms the basis for stratifying stands into mortality classes, which are used as both themes in a map and the basis of the field sampling design. Field measurements from 61 stands collected in the summer of 1992 indicate 15% of the original timber volume in the true fir zone died between 1988 and 1992. The resulting low standard error of 11% for this estimate indicates the utility of these mortality classes for detecting areas of high mortality. Also, the patterns in the estimated mean timber volume loss for each class follow the expected trends. The results of this project are immediately useful for fire hazard management, by providing both estimates of the degree of overall mortality and maps showing its location. They also indicate current remote sensing technology may be useful for monitoring the changes in vegetation that are expected to result from climate change.

*Center for Remote Sensing and Department of Geography, Boston University

Address correspondence to Scott A. Macomber, Ctr. for Remote Sensing, Boston Univ., 725 Commonwealth Ave., Boston, MA 02215.

Received 7 October 1993; revised 15 September 1994.

0034-4257/94/$7.00

655 Avenue of the Americas, New York, NY 10010

INTRODUCTION

Drought conditions during the years 1986–1992 resulted in considerable mortality of coniferous trees in the Sierra Nevada mountains of California. Drought weakened the trees, leaving them vulnerable to attack by insects such as the fir engraver beetle, *Scolytus ventralis* LeConte, and the Jeffrey pine beetle, *Dendroctonus jeffreyi* Hopk. (Smith, 1971; Ferrell, 1986; Swanson, 1992). The tree mortality encompasses a wide range of topographic, ecological, and geographic conditions and involves many species of conifers.

The primary goal of this investigation is to evaluate the potential for measuring and mapping the loss of conifers due to drought related effects using Landsat Thematic Mapper (TM) imagery. The approach presented here adapts current techniques for estimation of forest stand structure from TM imagery using the Li–Strahler geometric-optical canopy reflectance model (Li and Strahler, 1985). It also implements an automatic image segmentation scheme at the outset, providing an analysis of forest stand attributes based on regions instead of the more traditional per-pixel analysis. This exploratory investigation, designed both to locate and measure the amount of conifer mortality occurring between 1988 and 1991, was done for the Lake Tahoe Basin Management Unit in the Sierra Nevada mountains.

The ability to determine the level of insect damage to trees in the Basin would be beneficial to several aspects of area management, including timber harvest and salvage, fire prevention, wildlife management, and development planning. The methods used are expected to be applicable to other geographic areas, and to other situations where rapid and widespread change in canopy characteristics occur.

In order to determine mortality levels, estimates of stand structure derived from one date of imagery (9 July 1988) were compared with the same estimates for a later date (2 July 1991). Instead of attempting to detect the dead trees themselves, the change in canopy cover in each stand was the signal exploited. As trees die, their needles cease photosynthetic activity, changing the way they reflect solar radiation. The percent cover (the proportion of ground covered by living tree canopy) also decreases. Thus, in areas of significant mortality, a difference in living crown cover should be detectable. As a result, the detection of change and mortality was heavily dependent on the methods used to map crown cover.

Estimating mortality and tree loss for the entire Tahoe Basin was accomplished by stratifying the forest areas according to the degree of change (estimated by comparing the canopy model results from the 1988 and 1991 images). By sampling selected stands from each of 10 "mortality" strata in 1992, it was possible to estimate both the timber volume lost and the standard error of that estimate from 1988 to 1991 and 1992. The quality of the stratification and of the results were largely determined by the low standard error for the estimate of lost timber volume and the patterns of mortality in the strata.

Background

There has been a cooperative research agreement between the Boston University Center for Remote Sensing and the United States Forest Service Region 5 Remote Sensing Group (in Sacramento, California) since 1988. This research has focused on developing a set of new methods for mapping and inventorying forest vegetation using remote sensing and geographic information systems (GIS) with the goal of transferring the technology directly to their group (Woodcock et al., 1995). The research presented here is an extension of this project.

Traditional methods for measuring tree mortality in forests usually depend on aerial photography and/or sketch maps drawn by an observer in an aircraft. Wert and Roettgering (1968) combined an aerial survey and ground survey with a then new probability sampling technique to estimate damage from a Douglas-fir beetle epidemic. Articles by Byler (1978) and Smith et al. (1983) described the pest damage inventory in California (PDI), which used the same techniques for estimating timber mortality from dwarf mistletoe and insect infestations. Airphotos were acquired for random locations within a forest and manually photointerpreted for dead trees; then sites were randomly selected from the photos and measured on the ground. This provided estimates of tree mortality for a forest or group of forests and the standard deviation or standard error for the estimates. The success of this method depends on the acquisition of current, large scale aerial photographs, good photointerpretation of tree mortality, and the collection of field data from a large number of stands. The weaknesses of this method include a high standard error for the estimate [for example, $\pm 25\%$ for the estimate of board feet lost in northern California between June 1977 and June 1978 (Smith, 1983)], and the fact that maps cannot be produced showing the geographic distribution of mortality because of the sampling strategy used.

The Intermountain Region of the U.S. Forest Service (Region 4 includes Nevada, Utah, southern Idaho, and the Bridger-Teton National Forest in Wyoming) uses annual and biennial aerial detection surveys (ADS) to detect and monitor *highly visible* injury to trees caused by insect infestations (Beveridge and Knapp, 1984). A skilled aerial observer in an aircraft observes and identifies damage to trees, then uses symbols and colored pens to mark the location, extent, nature and severity of the damage on sketch maps, and then digitizes the information into a GIS database for further analysis. The products of this method include, but are not limited to, estimates of mortality by number of trees and total area affected. Using a GIS allows information to be analyzed in terms of various parameters, such as tree species, pest species, and year of death, and also allows for the production of maps showing the distribution of mortality. Currently, Region 4 estimates the annual loss of trees due to pests, but provides no measure of the robustness of the estimate such as the standard error (personal communication with Julie Weatherby, Forest Pest Management Office, USDA Forest Service, Boise Field Office, Idaho). This method is highly dependent on the skills and biases of the aerial observer, and the results would vary if more than one observer were used.

Several studies have shown that detection of forest damage using remotely sensed spectral data is possible because differences in spectral reflectance are generally correlated with differences in forest conditions (Rock et al., 1986; 1988; Vogelmann and Rock, 1988; Leckie, 1987; Westman and Price, 1988). The most common difficulty faced by researchers using the change detection methods discussed above may be that the difference between spectral signals of the dead trees and living or damaged trees must be greater than and distinct from differences in spectral signal caused by other factors. This separation of effects is made difficult by three general sets of factors. First, the variance among the signals of living trees in an image can be greater than the difference between living and dead trees due to several reasons. Leckie (1987) cites several factors limiting the success of using airborne MSS data for defoliation assessment of conifers, among them: radiometric distortion from atmospheric effects and topography, small spectral differences between damaged and undamaged trees, and a relatively large spectral variability of areas of similar defoliation due to differing forest stand characteristics. Topographic slopes are shown to cause more differences in spectral values between stands with similar damage levels than occurs between stands with different levels of damage. Second, when examining multitemporal data several factors external to the nature of a target object cause shifts in measured spectral reflectance of the same object at different times, in addition to those factors representing change in the object itself. These external factors, referred to as global effects, are radiometric distortions or shifts affecting most or all of an image, which are caused by three factors: atmospheric conditions, sun angle, and soil moisture (Singh, 1989). Third, geometric misregistration is known to impact adversely change detection, even when the same image is misregistered against itself at the subpixel level (Townshend et al., 1992).

The methods discussed in this article combine the techniques used in digital image processing of remotely sensed data with traditional sampling and field observation methods used by the U.S. Forest Service. Instead of using airphoto interpretation to identify dead trees in a forest, a form of image differencing is used to create a map of forest stands stratified by mortality. From these strata, a random sample of stands are chosen for field sampling. This approach eliminates photointerpretation for dead trees (and thereby the necessity of current, large scale airphotos), field observations from aircraft, and the intermediate step of producing sketch maps.

METHODS

Overview of Vegetation Mapping Procedures

Conceptually, the process of change detection can be thought of as a comparison of maps from two different dates. In practice, it can be a complex and difficult process. First, forest vegetation maps were produced using a set of methods involving the Landsat TM multispectral imagery, digital elevation data and field data. Descriptions of the entire classification, mapping, and inventory procedures are available in Woodcock et al. (1990; 1995).

The forest vegetation map was produced by first partitioning the satellite image into stands, using an automatic image segmentation procedure (Woodcock and Harward, 1992). The segmentation parameters produced stands ranging in size from about 2 ha to 20 ha. This minimum mapping unit size is necessary for Forest Service inventory maps which are used at a scale of 1:24,000. An unsupervised maximum likelihood classification procedure was used to create a per-pixel classification for the entire area. Each stand was then assigned to one land cover class, depending on the composition of the pixels in the per-pixel classification.

Regional forest types (which are broad conifer species associations) were modeled based on the relationship between conifer species and the terrain variables, elevation, slope, and aspect. Field observations were collected and used for calibrating a GIS model which predicts the regional type for each topographic situation. The model was implemented using GRASS, a public-domain geographic information system (USACERL, 1991). A description of this process as it was applied to the Stanislaus National Forest in California can be found in Macomber et al. (1991).

After the regional type of each conifer stand and the components' spectral signatures for each regional type were determined, the spectral data for each stand were sent to the forest canopy reflectance model. The model estimated, for each stand, the mean tree size (crown radius) and stand density (number of trees per acre). Using these parameters, it was possible to estimate the percentage of each stand covered by tree canopy, one component of the labels used in the final vegetation maps.

The Li–Strahler Invertible Forest Canopy Reflectance Model

The Li–Strahler model is designed to estimate the size and density of trees from remotely sensed images (Li and Strahler, 1985). It is a geometrical / optical model, and as such relies on the three-dimensional structure of the canopy as the primary factor influencing reflectance from the canopy. In this study, trees are modeled as an ellipsoid with r as the half crown width, b as the vertical half-axis, and h as the height from ground to the bottom of an ellipsoidal crown (Fig. 1). The model assumes that the satellite measurements (pixels) are larger than the size of individual tree crowns, but smaller than the size of forest stands. The signal received by the sensor is modeled as consisting of the sunlight reflected from tree crowns, the background, and the trees' shadows in the field of view of the sensor. Thus, the signal can be modeled as a linear combination of four components and their areal proportions:

$$S = K_g G + K_c C + K_t T + K_z Z, \qquad (1)$$

where S is the *brightness* value of a pixel, K_g, K_c, K_t, and K_z represent the areal proportions of sunlit background, sunlit crown, shadowed crown, and shadowed background, and G, C, T, and Z are the spectral signatures of the respective components (using digital number values).

Critical to this study is the "treeness" parameter, or m, which is defined as the mean of nr^2/A, where n is the poisson parameter, or the number of trees per pixel, and A is the area of a pixel. Conceptually, m is like a crown area index, and when multiplied by π would be equivalent to the proportion of the area covered by tree crowns if they did not overlap. The parameter m is important in the interface between the remote sensing signal and the forest parameters. Figure 2 shows four hypothetical component signatures in *brightness–green-*

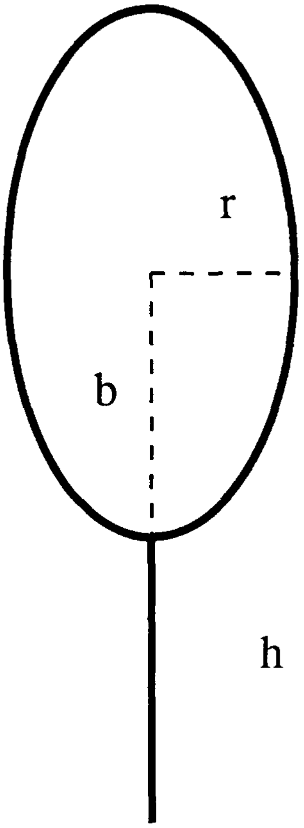

Figure 1. The tree geometry parameters of the Li–Strahler canopy model. *h* is the height from ground to the bottom of an ellipsoidal crown, *b* is the vertical half-axis, and *r* is half the crown width. The ratios r/b, h/b, and $b+h/r$ are used to describe crown geometry and are used as constants in the model.

ness space and a hypothetical "*m*-trajectory." When there are no trees in a stand, $m=0$ and the signal is simply the signature of the background (*G*). As trees are added and *m* increases, the signal moves toward a combined signature X_0, which is determined by the crown geometry and illumination conditions. The channels used in this graph (Fig. 2) and for the inversion of the canopy model are the standard *brightness* and *greenness* indices from the Tasseled Cap transformation, calculated using the published coefficients for Landsat TM (Crist and Cicone, 1984a, b). A piecewise linear contrast stretch was applied to each index to create single-byte bands.

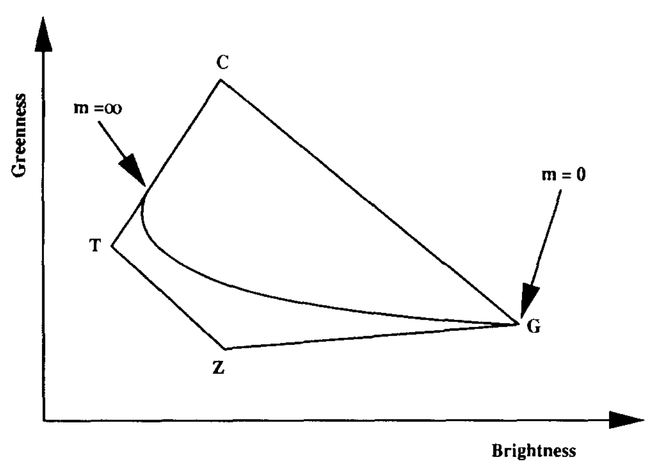

Figure 2. Hypothetical component signatures and *m*-trajectory in *brightness–greenness* space: sunlit tree crown (*C*), sunlit background (*G*), shaded tree crown (*T*), and shaded background (*Z*). $m=0$ at *G* and approaches infinity along the *T–C* line.

Field Measurement of Test Stands (Summer 1991)

Estimates of the spectral signatures in *brightness* and *greenness* for the model components [sunlit tree crown (*C*), sunlit background (*G*), shaded tree crown (*T*), and shaded background (*Z*)] are necessary for inversion of the canopy model (Fig. 2). They are estimated using a combination of field measurements and the spectral data extracted from the TM image for those stands.

During July and August 1991, test stands were selected from and hand-delineated on airphotos, and then visited by teams of trained field workers. Each stand was sampled using 16 variable-radius plots according to standard Forest Service techniques (Dilworth and Bell, 1971). Species and diameter-at-breast-height (DBH) were measured for each tree sampled. In addition, for two trees randomly selected at each point within the stand (the first live conifer trees to the east of north and west of south), the height of the tree, height to crown base, and crown diameter were measured. From these field data, several useful variables were estimated for each stand, including mean tree size (DBH), mean number of trees per acre, percent crown cover, and the tree geometry parameters needed for the model. These field data were critical for estimating component signatures for the model and were also valuable for evaluating alternative methods of detecting change.

Traditionally, only live trees are measured in sample plots. However, in this case any dead trees that appeared to have still been alive in 1988 were also measured and the apparent year of death recorded. As a result of sampling trees that had died since 1988, it was possible to reconstruct stand structure for both 1988 and 1991 and estimate the degree of mortality in each test stand during that period. A major component of the signatures of sunlit and shaded crown was the photosynthetically active chlorophyll present in needles, so that the year the needles appeared brown was more important than the year they died. Personnel from the Region 5 Office of Pest Management trained the field crews in the methods for determining the year of death using the physical condition of needles, branches, twigs, and bark and the presence or absence of insects. The pattern used to estimate death of the conifers was as follows. Trees with green needles were considered to be alive. Actually, fir trees (Abies spp.) take up to 1 year for the needles to lose their color so that some trees with green needles were actually dead but not yet brown. Trees with most or all of their needles brown but still on the tree were determined to be dead for 1 year. Trees that had lost most of their needles and some smaller twigs were dead for 2 years. Trees with no needles remaining and most of the smallest twigs missing were dead 3 years. Trees with no needles, most of the small branches missing, and some decaying bark were dead 4 years. Trees with no needles, most branches missing, and bark decayed were dead 5 years.

Change Detection Methods

The approach used to detect change measured the decrease in overall crown cover between two dates, not the signature for dead trees. Estimates of crown cover from the Li–Strahler model were compared for each conifer stand between the two dates. There were a number of issues and steps involved in executing that comparison.

A critical issue in any multidate comparison is accurate image geometric registration between the dates (Townshend et al., 1992). The method used to register the images was the collection of 55 ground control points, acquired from the images within the bounds of the management unit, which were used in a rubber-sheeting program with a third-order polynomial fit. This resulted in a mean-squared error of less than 0.3 pixels for the registration. Although this method was more time-consuming and tedious than some automated registration algorithms, it allowed for considerable control of the results. The use of automatic image-matching based approaches was considered and rejected, primarily because they assume little change in the scene between dates. The widespread change in the landscape due to drought made such an assumption inappropriate.

For the purposes of using the canopy model for change detection, estimates of *brightness* and *greenness* for each of the four component signatures were needed for both dates of imagery. Three approaches were possible. First, one could standardize radiometrically the *brightness* and *greenness* values between the two dates. The problem with this approach was that there were significant changes in the scene between dates and there was no basis for separating changes in the images due to global effects and those resulting from change in the scene. Second, one could estimate the component signatures for each date of imagery separately. This approach was not selected as it could introduce a convolving effect into the change detection. The third approach, chosen for this study, was to use the same set of component signatures for both dates. The principal advantage of this approach is a consistent set of signatures across dates, with the disadvantage resulting from the shift in *brightness* and *greenness* values between dates.

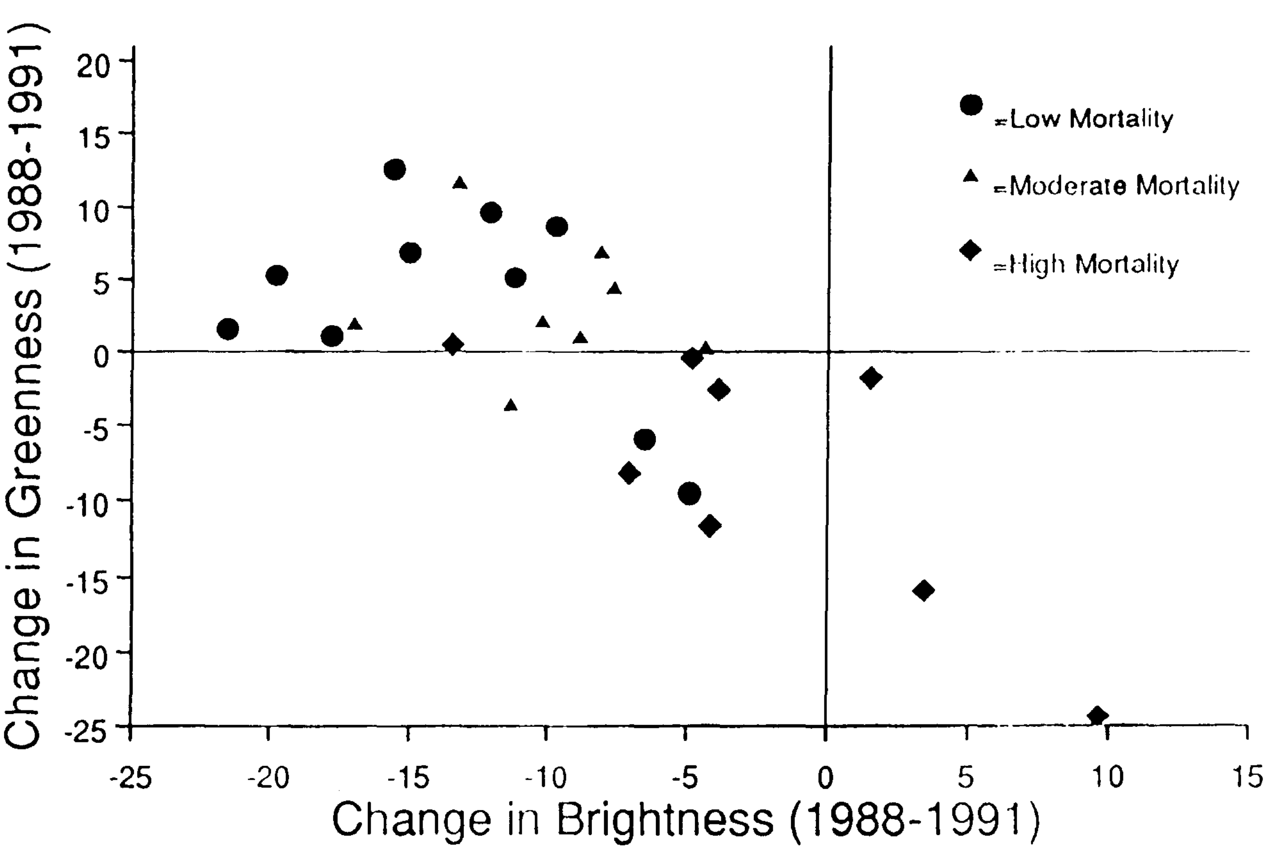

Figure 3. Change in brightness and greenness transforms from 1988 to 1991, by mortality class.

Before applying the canopy model to the test stands, the image data from the two dates were examined and compared. The difference between mean *brightness* values were plotted against the difference between mean *greenness* values for each test stand to evaluate the changes in *brightness* and *greenness* values between dates (Fig. 3). The test stands were stratified into three levels of mortality to help separate effects associated with change due to mortality from global changes in the image. Based on Figure 3, it was apparent that there were global differences between dates, as the stands exhibiting low degrees of mortality were concentrated in the upper left quadrant, not at the origin of the axes. However, it was also apparent there was a clear trend between mortality and changes in *brightness* and *greenness*, with the changes in the directions anticipated for a decrease in forest cover associated with mortality; the high mortality stands tended to be brighter and less green than the low mortality stands.

Figure 4 is a graph of the relationship between change in basal area as measured in the field and change in m-values as estimated by the model. The graph illustrates four points: First, there is a strong relationship between changes in m-values and changes in basal area ($r^2 = 0.68$, significant at the 0.0001 level). While the relationship is strong, there is a fair amount of noise in stands with little change in basal area. Second, it shows the direction of change matches expectations, meaning that stands with reduced basal area due to mortality tend to exhibit lower m-values from the 1991 image. Third, the entire relationship is shifted to the right of

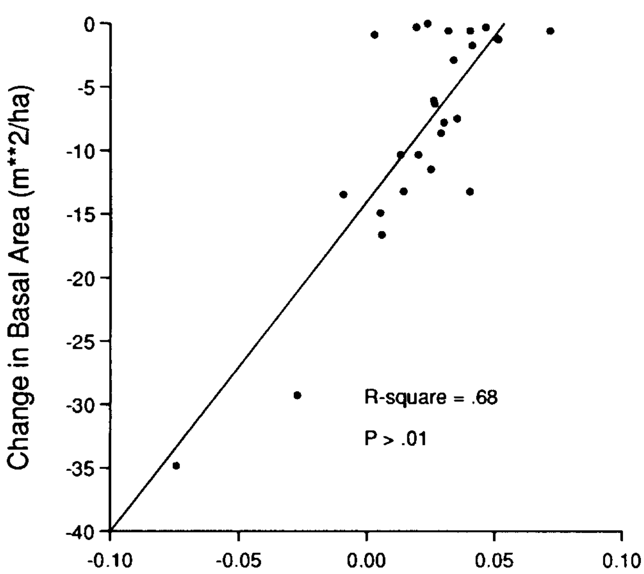

Figure 4. Change in m-value (from the model) plotted against the change in basal area (m^2 / ha) measured in the field for the 1991 test stands. r^2 is 0.68, significant at the 0.01 level ($n = 25$).

zero due to the global differences in *brightness* and *greenness* values between dates. In other words, the estimated m-value can increase slightly between dates but still indicate a reduction in basal area. This effect was expected because the same signatures were used for both dates. Finally, no stand showed an increase in basal area from 1988 to 1991. When recreating the past condition of the stands, basal area was decreased by subtracting dead trees from the stands in the year their needles turned brown, but it was too difficult to estimate the increase in size of individual trees for each year and thus which trees would still be large enough to be counted as part of the field sample for each point at each year. Thus, the growth of living trees had to be ignored.

The difference between m-values for the two dates provided a continuous measure of change for each conifer stand in the study area and was used to sort the stands into three sampling strata. Cutoff points for the strata were determined by placing 50% of the conifer stands in the low change class, 40% in moderate change, and 10% in high change. These divisions concentrated the samples in the stands with higher mortality.

Both the conifer mortality and the ability to estimate mortality using the model were affected by the percent cover of the stands. Mortality appeared significantly higher in denser stands (possibly due to competition for limited water and / or insect preference), and change in m-value had a weaker relationship with actual change in the less dense stands. Therefore, percent crown cover was also used as a basis for stratification. Sorting the stands into three equal strata spread the samples over the full range of cover conditions. Combining these two factors resulted in nine strata.

Maps of the few sites where salvage operations had occurred since 1988 were provided by the local Forest Service Supervisor's Office, and then digitized. Separating the salvaged stands from the rest of the forest aided the analysis of the trends being examined. Not only did salvaged stands have a dramatic decrease in crown cover, but they were also unlikely to be labeled as "conifer" in the classification of the 1991 image. However, they needed to be sampled for inventory purposes so that these stands became a 10th stratum. A simple GIS operation was used to assign each conifer stand to the correct mortality stratum (Table 1).

Field Measurement of Test Stands (Summer 1992)

Field measurements in stands randomly selected from the 10 strata were carried out in the summer of 1992. These were done in a manner similar to the work done in 1991, with a few significant differences. First, the test stands were selected randomly from the segmented image instead of being manually selected on the airphotos. Six stands were measured in each of the 10 strata (except stratum H3 had seven stands) for a total of 61

Table 1. Mortality Strata Labels and Definitions

Stratum Label	*Cover Class*	*Mortality Class*
L1	Low	Low
L2	Low	Moderate
L3	Low	High
M1	Moderate	Low
M2	Moderate	Moderate
M3	Moderate	High
H1	High	Low
H2	High	Moderate
H3	High	High
S3	Low	Salvage

stands. Second, no tree heights or crown geometry parameters were measured since these were only necessary for calibrating the canopy model. Third, each stand was sampled with a higher spatial frequency, in an attempt to improve sampling of mortality, which tends to occur in small groups of trees within a stand. The number of points was increased from 16 per stand to 1 point per pixel, with a minimum of 20 and a maximum of 82 points per stand. The points were laid out in a regular grid pattern, spread evenly over the area of the stand starting with a randomly located first point. While more points were visited in each stand, the data required at each point could be quickly collected. Salvage stands were measured by estimating DBH from the stumps and measuring the distance from the cluster point to the center of the stump to determine if each tree should be included.

For forest management and inventory purposes, the amount of trees in a forest is usually measured in either units of basal area or timber volume. However, for brevity, this article includes only the full results for basal area. Both were used in this study and are reported in Macomber (1995). Estimates of basal area for an area are computed by multiplying the mean basal area for each stratum (as derived from field samples) times the area for the stratum, and then summed across strata. The quality of the stratification is determined by low standard errors in the estimates of basal area for each stratum, which are used in turn to estimate the standard error of the estimate of the basal area for the entire forest. In addition to estimating the mean basal area, it is possible to estimate the mean of the basal area *loss* for each stratum and use the same procedures to estimate total timber volume loss. The standard error of the timber volume loss can then be used to evaluate the quality of the estimate.

RESULTS

Analysis of the 1992 field data provided estimates of the basal area of living and dead conifer trees, for each of the years 1988–1991. Evaluating this method of change detection focused on the change in basal area from 1988 to 1991 because basal area closely correlates to percent cover and these are the dates of the imagery. In addition, the patterns of change in basal area can be examined either as the total amount of change or as the percentage change from the original.

Results indicate that using both the change in m-value and the cover classes for stratification were useful for estimating mortality. Figure 5 shows change in total basal area (5a) and percent of basal area (5b) for each of the nine main strata. Lines connect the means for the levels of change of the three cover categories. These graphs reveal three distinct patterns in the strata. First, within each cover class, the mortality classes sort as expected; that is, the high mortality class has the greatest mortality, while the moderate and low mortality classes show less mortality. Similarly, the low cover classes show less mortality than the high cover classes. These main patterns hold for both total basal area lost and percent of basal area lost. Second, percent change proves more useful for comparing the levels of mortality in the low cover class because in the low cover class a relatively small total loss in basal area can be a significant percent loss for a stand. Third, these graphs show that mortality varies as a function of percent cover. The total basal area loss in the low change class for high cover is greater than the high mortality class for low cover. Therefore, using cover as a second variable in the stratification helped detect change and illustrate the patterns in mortality as distributed across the landscape.

Based on the random sampling of the cover and mortality strata, it is possible to estimate the total basal area loss for the Lake Tahoe Basin (Tables 2a, 2b, and 2c). It is important to keep in mind that these tables reflect basal area and mortality only for mixed conifer, red fir, and subalpine stands and do not include Jeffrey pine stands. Each table gives the means and standard errors for each stratum and their respective areas. Using this data, it is possible to estimate both the total loss for the entire area and the standard error of that estimate, E:

$$E = \frac{\sqrt{s^2_{(\bar{y}_{st})}} * A}{V} * 100, \qquad (2)$$

where E is the standard error for the estimate of the total expressed as a percent of the total, A is the total area, V is the estimate of the total volume, and $s^2_{(\bar{y}_{st})}$ is the sum of the contributions to variance (Cochran, 1977, Eq. (5.13), p. 95).

For basal area, the mortality estimate between 1988 and 1991 is a total of 260,000 m^2, or 4.6 m^2/ha, which is nearly 10% of the total basal area alive in 1988 (Table 2b). By 1992, mortality increased to 357,000 m^2, or more than 13% of the total (Table 2c). The standard

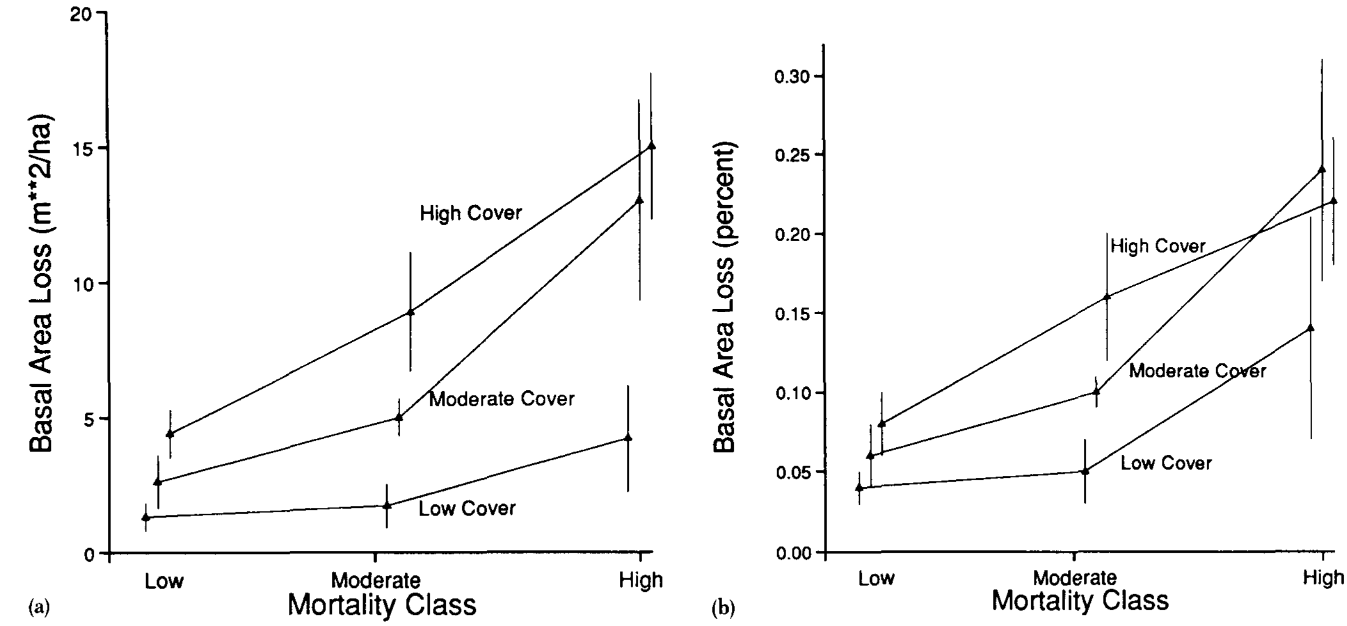

Figure 5a and 5b. Mean and standard error of basal area loss by strata. Lines connect strata belonging to the same cover classes. Basal area is in units of m^2 / ha for 5a, and in percent of the original strata which died for 5b. Error bars represent the standard error of the estimate. Points are shifted slightly to permit discrimination of error bars.

error for this estimate is less than 9% based on 61 samples. How then to interpret the standard errors of the estimates? One approach is to use the U.S. Forest Service standards for inventory of live trees, which require less than a 10% standard error for the estimate of total timber volume and 20% within individual strata. Since it is much more difficult to inventory dead trees than live trees, it is impressive these results for dead trees meet the normal standards required for inventory of live trees.

Change in basal area is most useful for evaluating the utility of the Li-Strahler model for detecting change but the change in timber volume is most useful for evaluating the utility of the Li-Strahler model for estimating the information desired by forest managers. The main patterns seen in the basal area analysis are also evident for timber volume. The full results of the timber volume analysis are found in Macomber (1995). For timber volume, the total estimate of loss between 1988 and 1991 is 2.2 million m^3. By 1992, this increased to

Table 2a. Inventory Summary for Basal Area Lake Tahoe Basin Management Unit—Live Trees (1988)

Stratum	*Basal Area (m^2 / ha)*	*Standard Error*	*Number of Stands*	*Hectares (× 1000)*	*Area Weight*	*Total Basal Area (× 1000)*	*Contribution to Variance*
L1	37.0	4.4	6	5.4	0.095	199	0.173
L2	35.8	5.8	6	9.8	0.173	351	0.997
L3	30.3	5.2	6	1.4	0.024	42	0.016
M1	44.8	2.5	6	11.1	0.195	495	0.244
M2	48.0	7.1	6	6.6	0.117	319	0.692
M3	53.7	4.0	6	1.1	0.019	58	0.006
H1	56.1	6.1	6	15.0	0.265	841	2.579
H2	55.3	4.4	6	2.8	0.050	155	0.047
H3	67.6	3.9	7	1.8	0.031	120	0.015
S3	48.1	4.9	6	1.7	0.030	81	0.022
Total			61	56.6	1.000	2661	4.791

Estimates for The Entire Forest

Basal area live in 1988 (*V*)	2,661,000 m^2
Total area (*A*)	56,600 ha
Average	47 m^2 / ha
Variance ($s^2_{(\bar{y}_{st})}$)	4.79
Standard error (*E*)	4.65%

3 million m^3 with a standard error for the estimate of 11%. While this slightly exceeds the standard for live trees, it supports the idea that effective inventory of mortality with remote sensing is possible in these types of forest. According to David Schultz, an entomologist for the U.S. Forest Service in California, "background mortality during periods of seminormal precipitation will run around 0.1 trees per acre per year, or about 0.5% of the volume per acre per year" (personal communication) or about 2% over a 4-year period. Note that these figures are broad averages, for northern California forests, which apply over large areas. The loss of 3 million m^3 in timber volume corresponds to 15% mortality over 4 years, which helps illustrate the magnitude of the problem in the Lake Tahoe Basin.

To further investigate the methods used to map and inventory mortality, we plotted loss in basal area as a function of change in *m*-values (Fig. 6a) for the 1992 test stands. The overall pattern of the stands is similar to that seen in Figure 4 (from the 1991 field stands),

Table 2b. Inventory Summary for Basal Area Mortality Lake Tahoe Basin Management Unit—Dead Trees (1988–1991)

Stratum	*Basal Area (m^2/ha)*	*Standard Error*	*Number of Stands*	*Hectares (×1000)*	*Area Weight*	*Total Basal Area (×1000)*	*Contribution to Variance*
L1	1.3	0.5	6	5.4	0.095	7	0.002
L2	1.7	0.8	6	9.8	0.173	17	0.017
L3	4.2	2.0	6	1.4	0.024	6	0.002
M1	2.6	1.0	6	11.1	0.195	29	0.035
M2	5.0	0.7	6	6.6	0.117	33	0.007
M3	13.0	3.7	6	1.1	0.019	14	0.005
H1	4.4	0.9	6	15.0	0.265	66	0.061
H2	8.9	2.2	6	2.8	0.050	25	0.012
H3	15.0	2.7	7	1.8	0.031	27	0.007
S3	21.9	3.3	6	1.7	0.030	37	0.010
Total			61	56.6	1.000	260	0.158

Estimates for The Entire Forest

Basal area mortality by 1991 (V)	260,000 m^2
Total area (A)	56,600 ha
Average	4.6 m^2/ha (~10%)
Variance ($s^2_{(\bar{y}_{st})}$)	0.16
Standard error (E)	8.65%

Table 2c. Inventory Summary for Basal Area Mortality Lake Tahoe Basin Management Unit—Dead Trees (1988–1992)

Stratum	*Basal Area (m^2/ha)*	*Standard Error*	*Number of Stands*	*Hectares (×1000)*	*Area Weight*	*Total Basal Area (×1000)*	*Contribution to Variance*
L1	2.0	0.8	6	5.4	0.095	11	0.007
L2	2.4	1.0	6	9.8	0.173	24	0.028
L3	5.6	3.1	6	1.4	0.024	8	0.005
M1	4.5	1.5	6	11.1	0.195	49	0.082
M2	5.9	0.9	6	6.6	0.117	39	0.012
M3	15.3	3.5	6	1.1	0.019	17	0.004
H1	6.3	1.5	6	15.0	0.265	94	0.156
H2	13.2	2.1	6	2.8	0.050	37	0.011
H3	21.3	2.4	7	1.8	0.031	38	0.006
S3	23.7	3.2	6	1.7	0.030	40	0.009
Total			61	56.6	1.000	357	0.320

Estimates for The Entire Forest

Basal area mortality by 1992 (V)	357,000
Total area (A)	56,600
Average	6 m^2/ha (~13%)
Variance ($s^2_{(\bar{y}_{st})}$)	0.32
Standard error (E)	8.96%

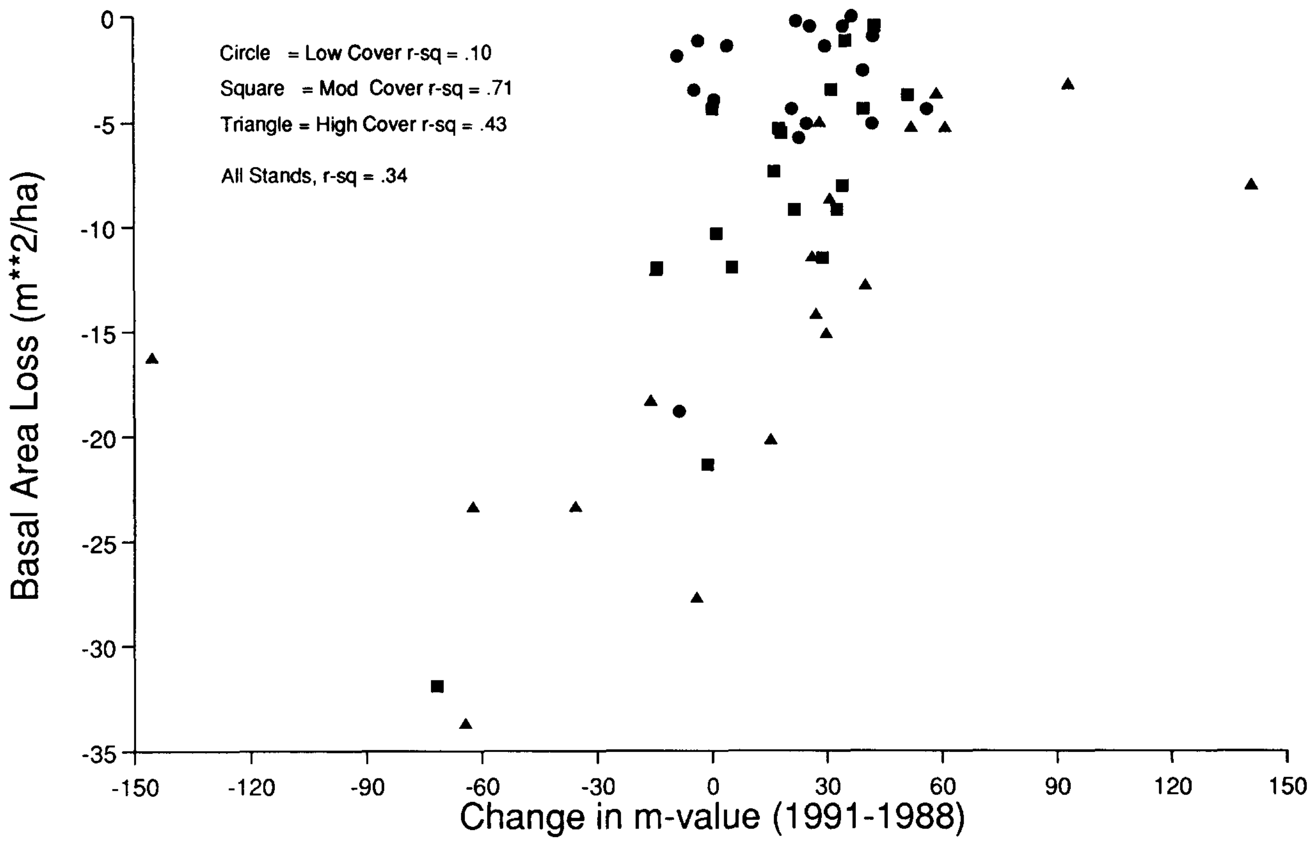

Figure 6. Basal area loss (in m^2/ha) as a function of change in m-value for the 1992 test stands. r^2 is 0.34 for all stands, 0.10 for stands with low cover, 0.71 for stands with moderate cover, and 0.43 for stands with high cover.

although the strength of the relationship is not strong. The r^2 is 0.34, significant at the 0.01 level, with a slope of 0.12, but there is considerable spread around the regression line. The patterns and the strength of the relationship between change in m-value and change in basal area are different for the low cover class as compared to the moderate and high cover. This difference can be seen in the graph. The low cover class has an r^2 of 0.10, which is not significant at the 0.10 level and a slope of only 0.07. The moderate and high cover classes have r^2s of 0.71, and 0.43, respectively. This demonstrates the interaction of cover and mortality and the importance of using both parameters for stratification. However, based on these results, it may be sufficient to use two strata for cover, separating the low cover stands from the rest.

DISCUSSION

The results of the mortality inventory for the entire Lake Tahoe Basin Management Unit, presented in Table 2, demonstrate the utility of this method. The patterns in mortality for the various strata (Fig. 5) and the low standard error for the estimate are the basis for that interpretation. However, a significant question concerns the level at which the estimates of mortality can be used.

Should the continuous estimate of mortality be used or only the stratum level, and how dependable are the estimates for individual stands? The low r^2 for the relationship between the change in m-value and change in basal area (Fig. 6) suggests that the continuous estimates for individual stands are not highly reliable. However, there are several possible reasons why the overall relationship of the 1992 test stands ($r^2 = 0.34$) is not as strong as the 1991 test stands ($r^2 = 0.69$). The most obvious reason is the two points at the extreme left and right sides of the graph. If these two points are removed, the overall r^2 improves to 0.48 and r^2 for the high cover class improves from 0.43 to 0.73. The point at the far left has a measured loss of 17 m^2/ha, which places it in the high mortality stratum. However, the large negative change for m-value would have predicted a much greater loss if a continuous estimate of mortality were used. The stand shows a large bright area of several pixels in the 1991 image where there was none in the 1988 image, which may explain the decrease in m-value. If mortality is concentrated in one small area, it may be missed by field measurements. The point at the far right has a large positive change in m-value and therefore was placed in the low mortality category, but the loss of 14 m^2/ha would make the moderate mortality class more appropriate. This stand is bounded on two sides by lush, wet meadows. The slight, but inevitable, shifting between the two images could result in the inclusion of some signal from either or both of the meadows in the stand, which would explain the large increase in m-value. Neither of these stands should be eliminated from the analysis nor should any pixels be removed from them. The stands and the mixed pixels are not outliers but are representative of the types of problems inherent in this method.

There were also effects associated with the different methods used to select stands each year. For the 1991 field data, stands were hand delineated on airphotos, but the 1992 stands were delineated using an automated image segmentation of the Landsat TM image, and then randomly selected. The hand-delineated stands had simpler shapes and were more compact than the segmented stands and were therefore much less susceptible to problems of misregistration. Analysis of shape parameters showed the mean perimeter to area ratio for the hand-delineated stands was 0.55, while the same ratio for the segmented stands was nearly double that, at 0.93. The increase in perimeter for a given area increased the effects of even minor misregistration.

A significant consideration for change detection is the scale for comparing model results. As mentioned earlier, the Li–Strahler model is inverted for groups of pixels or stands, rather than on a per-pixel basis. Comparing stand attributes instead of pixel attributes also provides an advantage in overcoming problems of misregistration. Experience with the registration process shows that it is impossible to register two images perfectly. For example, in several places a road appears in one image as a bright line only a single pixel wide (the signal is primarily from the road) while in the other image, the same road appears less bright and two pixels wide (each pixel contains some signal from the road and some signal from the adjacent land). This difference is due to slight shifts in the area sensed between dates. Despite the fact that perfect registration is not possible, it can be quite good if time and care are taken. By enlarging the unit of measurement from the single pixel to the stand, the effects of misregistration are reduced.

CONCLUSIONS

This research demonstrates that it is feasible to map and inventory changes in forest canopy cover using multitemporal remotely sensed imagery and to produce useful results in a timely fashion. Changes in vegetation affect management of land use, fire, wildlife, and timber. Resource managers need this information to plan and act effectively. This method is more useful for resource managers than traditional methods because it provides both the statistical results of an inventory, with a high level of accuracy, and also maps showing the geographic distribution of mortality patterns. These maps are produced at various scales: as separate quadrangle sheets at 1:24,000 (most useful for the field), and at one map for the entire forest. Since they are digital, they can be included in a GIS database for analysis using auxiliary data layers.

The results of the forest wide mortality inventory show a 15% loss of timber volume from the mixed conifer and red fir zones of the Lake Tahoe Basin between 1988 and 1992. The standard error of 11% demonstrates the validity of using these methods for estimates at the forest wide scale. At the stand level, results are less clear. The overall r^2 of 0.34 for basal area loss as a function of change in m-value is lower than anticipated, but trends within cover classes are generally better. This demonstrates the importance of using crown cover when estimating mortality. The low r^2 is at least partially due to the nature of the automatic image segmentation. The inclusion of small areas with different cover types, which are too small to stand alone, within larger stands may affect the results of the change detection. Minor levels of misregistration are likely a key factor in limiting the ability to accurately measure change at the stand level.

This research was funded by a cooperative research agreement between the Boston University Center for Remote Sensing and the U.S. Forest Service, Region 5. The authors wish to thank the USDA Forest Service personnel from the Remote Sensing Lab in Sacramento, the Forest Pest Management Office, and the Forest Supervisor's Office of the Lake Tahoe Basin Management Unit who helped in countless ways. Special thanks are due Jack Levitan, Ralph Warbington, Kevin Casey, Lisa Mann-Levien, Kama Kennedy, Tina Terrell, John Pronos, John Neisess, and Joe Oden. We would also like to thank John Collins, Sue Dorfman, Vida Jakabhazy, Soren Ryherd, Alan Strahler, and Xiaowen Li for their help in the field and lab.

REFERENCES

Beveridge, R. L., and Knapp, K. A. Report No. 84-8, (1984), Detection and dissemination of forest pest data in the intermountain region utilizing aerial detection surveys and computer mapping systems, USDA Forest Service Intermountain Region, Forest Pest Management Office, Boise, ID, October.

Byler, J. W. (1978), The pest damage inventory in California, presented at the Symposium on Dwarf Mistletoe Control through Forest Management, Berkeley, CA, 11–13 April, pp. 162–171.

Cochran, W. G. (1977), *Sampling Techniques*, 3rd ed., Wiley, New York.

Crist, E. P., and Cicone, R. C. (1984a), A physically-based transformation of Thematic Mapper data—the TM Tasseled Cap, *IEEE Trans. Geosci. Remote Sens.* GE-22(3):256–263.

Crist, E. P., and Cicone, R. C. (1984b), Application of the

Tasseled Cap concept to simulated Thematic Mapper data, *Photogramm. Eng. Remote Sens.* 50(3):343–352.

Dilworth, J. R., and Bell, J. F. (1971), *Variable Probability Sampling—Variable Plot and Three-P*, Oregon State University Book Stores, Corvallis, 1978.

Ferrell, G. T. (1986), Fir engraver, Forest Insect and Disease Leaflet 13, U.S. Department of Agriculture Forest Service, Washington, DC.

Leckie, D. G. (1987), Factors affecting defoliation assessment using airborne Multispectral Scanner data, *Photogramm. Eng. Remote Sens.* 53(12):1665–1674.

Li, X., and Strahler, A. H. (1985), Geometric-optical modeling of a conifer forest canopy, *IEEE Trans. Geosci. Remote Sens.* GE-23(5):705–721.

Macomber, S. A. (1995), Remote sensing of forest structure and change, Ph.D. dissertation, Boston University, Department of Geography, January.

Macomber, S., Woodcock, C. E., Warbington, R., and Casey, K. (1991), Modeling species associations for vegetation maps using terrain rules, in *Proceedings, Grass Users 1991 Conference*, Center for Environmental Design Research, Univ. of California, Berkeley, pp. 137–147.

Rock, B. N., Vogelmann, J. E., Williams, D. L., Vogelmann, A. F., and Hoshizaki, T. (1986), Remote detection of forest damage, *Bioscience* (Jul. / Aug.).

Rock, B. N., Hoshizaki, T., and Miller, J. R. (1988), Comparison of *in situ* and airborne spectral measurements of the blue shift associated with forest decline, *Remote Sens. Environ.* 24:109–127.

Singh, A. (1989), Digital change detection techniques using remotely-sensed data, *Int. J. Remote Sens.* 10(6):989–1003.

Smith, R. H. (1971), Jeffrey pine beetle, Forest Pest Leaflet No. 11, FR, USDA, Forest Service, April 1971.

Smith, R., Jr., Byler, J., Wood, R. E., Caylor, J., Hoskins, W., and Scharpnack, N. (1983), Pest damage inventory, a method for measuring pest-caused tree mortality in California, USDA Forest Service, Methods Application Group, Fort Collins, CO, 15 pp.

Swanson, J. (1992), State of the Lake Tahoe Forest today, what is the diagnosis?, in *For. Health Rep.*, 1(1).

Townshend, J. R., Justice, C. O., Gurner, C., and McManus, J. (1992), The impact of misregistration on change detection, *IEEE Trans. Geosci. Remote Sens.* 30(5):1054–1060.

USACERL (1991), *GRASS 4.0 User's Reference Manual*, U.S. Army Corps of Engineers Construction Engineering Research Laboratories, Champaign, IL, July.

Vogelmann, J. E., and Rock, B. N. (1988), Assessing forest damage in high-elevation coniferous forests in Vermont and New Hampshire using Thematic Mapper data, *Remote Sens. Environ.* 24:227–246.

Wert, S. L., and Roettgering, B. (1968), Douglas-fir beetle survey with color photos, *Photogramm. Eng.* (Dec.):1243–1248.

Westman, W. E, and Price, C. V. (1988), Spectral changes in conifers subjected to air pollution and water stress: experimental studies, *IEEE Trans. Geosci. Remote Sens.* 26(1):11–21.

Woodcock, C. E., and Harward, V. J. (1992), Nested-hierarchical scene models and image segmentation, *Int. J. Remote Sens.* 13(16):3167–3187.

Woodcock, C. E., Jakabhazy, V., Macomber, S., Ryherd, S., Strahler, A. H., and Wu, Y. (1990), Timber inventory using Landsat Thematic Mapper imagery and canopy reflectance models, in *23rd International Symposium on Remote Sensing of Environment*, Bangkok, Thailand, April, Vol. 2, pp. 937–948.

Woodcock, C. E., Collins, J., Gopal, S., et al. (1995), Mapping forest vegetation using Landsat TM imagery and a canopy reflectance model, *Remote Sens. Environ.* 50:240–254.